Organic & Biomolecular Chemistry

Cite this: *Org. Biomol. Chem.*, 2012, **10**, 3398

www.rsc.org/obc

PAPER

ortho-Phenylene oligomers with terminal push–pull substitution†‡

Jian He, Sanyo M. Mathew, Sarah D. Cornett, Stephan C. Grundy and C. Scott Hartley*

Received 20th December 2011, Accepted 29th February 2012
DOI: 10.1039/c2ob07146k

ortho-Phenylenes are an emerging class of helical oligomers and polymers. We have synthesized a series of push–pull-substituted *o*-phenylene oligomers (dimethylamino/nitro) up to the octamer. Conformational analysis of the hexamer using a combination of low-temperature NMR spectroscopy and *ab initio* predictions of ^{1}H NMR chemical shifts indicates that, like other *o*-phenylenes, they exist as compact helices in solution. However, the substituents are found to have a significant effect on their conformational behavior: the nitro-functionalized terminus is 3-fold more likely to twist out of the helix. Protonation of the dimethylamino group favors the helical conformer. UV/vis spectroscopy indicates that the direct charge-transfer interaction between the push–pull substituents attenuates quickly compared to other conjugated systems, with no significant charge-transfer band for oligomers longer than the trimer. On protonation of the dimethylamino group, significant bathochromic shifts with increasing oligomer length are observed: the effective conjugation length is 9 repeat units, more than twice that of the parent oligomer. This behavior may be rationalized through examination of the frontier molecular orbitals of these compounds, which exhibit greater delocalization after protonation, as shown by DFT calculations.

Introduction

Abiotic oligomers and polymers that adopt well-defined secondary structures are currently of great interest as mimics of biomolecules and in materials science and nanotechnology.[1–6] Molecules that fold into helices (the most common motif[6]) have been used in molecular recognition[7–12] and may exhibit mechanical actuation[13–15] or desirable chiroptical properties.[16–18] Because of their three-dimensional structures, these architectures can also be used as molecular scaffolding for the organization of functional moieties in space (*e.g.*, chromophores).[19,20] Nevertheless, while a variety of different folded architectures have been reported, there remain many very simple structural motifs for folding that have yet to be thoroughly explored.

The *ortho*-phenylenes represent a fundamental class of conjugated polymers (or oligomers), but they have received only limited attention[21–25] compared to other systems because steric twisting limits their π-system delocalization. However, they have recently emerged as a new class of helical oligomers. For example, Fukushima and Aida have demonstrated a remarkable *o*-phenylene octamer that exhibits spontaneous resolution of a helical conformation in the solid state, along with a series of monodisperse *o*-phenylenes up to the [48]-mer.[26] Our own group has been exploring the electronic structures and conformational behavior of simple *o*-phenylene oligomers.[27–30] As expected, delocalization in an *o*-phenylene is substantially attenuated (*e.g.*, compared to *para*-phenylenes) due to their twisted structures: the effective conjugation length of the parent (unsubstituted) series is quite short ($n_{ecl} \approx 4$).[29] The conjugation length appears to be sensitive to substitution, however, as functionalization with methoxy groups increases it significantly ($n_{ecl} \approx 8$).[27] We have also shown that the *o*-phenylenes have a strong preference for a compact stacked helical conformation in solution, with the only significant conformational variability occurring at the ends of the chains.[28,29]

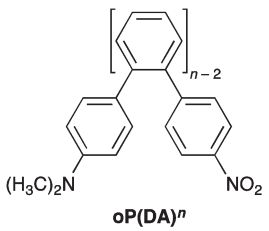

oP(DA)^{n}

To continue our investigation of the electronic and conformational properties of *o*-phenylenes, we decided to prepare the homologous series of oligomers **oP(DA)^{n}**, which are end-functionalized with donor and acceptor groups (dimethylamino and

Department of Chemistry & Biochemistry, Miami University, Oxford, OH 45056, USA. E-mail: scott.hartley@muohio.edu; Fax: +1 (513) 529–5715; Tel: +1 (513) 529–1731

†This article is part of an *Organic & Biomolecular Chemistry* web theme issue on Foldamer Chemistry.

‡Electronic supplementary information (ESI) available: supplemental figures referred to in the text; NMR spectra of **oP(DA)^{6}**; energies for optimized geometries; synthetic details for **oP(DA)^{2}**, **oP(DA)^{3}**, **oP(D)^{4}**, and **oP(A)^{4}**; NMR spectra of all novel compounds; Cartesian coordinates for optimized geometries; and complete ref. 58. See DOI: 10.1039/c2ob07146k

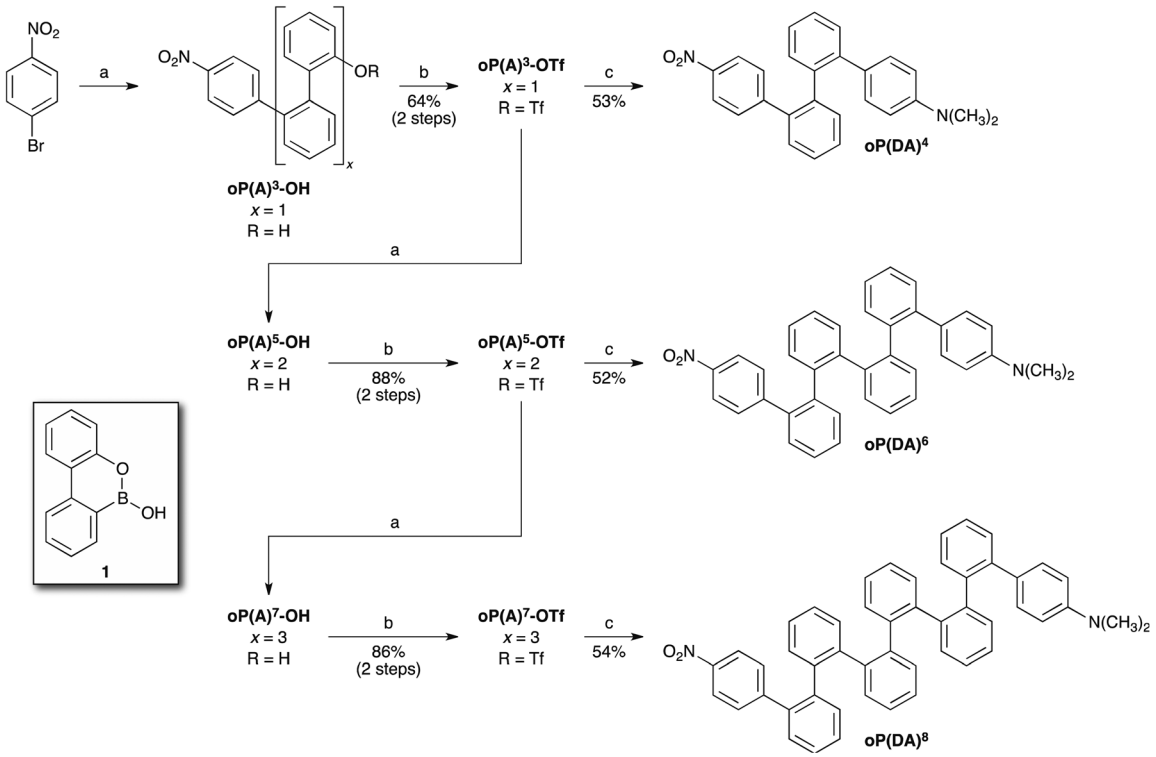

Scheme 1 Reagents and conditions: (a) **1**, $Pd(OAc)_2$, SPhos, K_3PO_4, THF/H_2O (4/1), 90 °C; (b) Tf_2O, pyridine, CH_2Cl_2, 0 °C to r.t.; (c) 4-(dimethylamino)phenylboronic acid, $Pd(OAc)_2$, SPhos, K_3PO_4, THF/H_2O (4/1), 90 °C.

nitro, respectively). In general, such "push–pull" oligomers are of interest as functional materials with desirable linear and nonlinear optical properties.[31] This series of compounds allows us to probe both electronic effects in the *o*-phenylenes and substituent effects on their conformational behavior. We show here that direct electronic interaction through the *o*-phenylene backbone is limited, but a long effective conjugation length is restored on protonation of the dimethylamino groups. The substituents are also found to have a significant effect on the conformational behavior of the structures.

Results and discussion

Synthesis

Our synthetic approach to the **oP(DA)^n** series, shown in Scheme 1, uses our previously developed strategy,[27,29] which is based on Manabe and Ishikawa's oligophenylene synthesis using phenols as masked triflates.[32,33] Briefly, the key building block for our synthesis is boroxarene **1**, which is readily obtained by treatment of 2-phenylphenol with boron trichloride.[34] Suzuki coupling[35] of **1** with 1-bromo-4-nitrobenzene affords **oP(A)^3-OH**, which can be activated toward further coupling reactions by triflation to give **oP(A)^3-OTf**. The oligomer can be terminated at this point by Suzuki coupling with 4-(dimethylamino)phenylboronic acid, giving **oP(DA)^4**, or extended by coupling with another equivalent of **1**, giving **oP(A)^5-OH**. This sequence is then repeated to give the higher oligomers **oP(DA)^6** and **oP(DA)^8**. Syntheses of the short oligomers considered here, **oP(DA)^2** and **oP(DA)^3**, are described in the ESI.‡

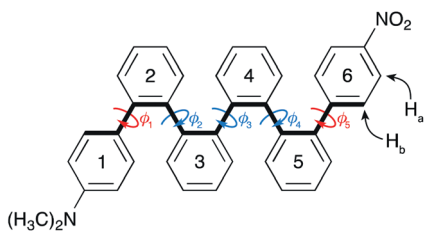

Fig. 1 Ring and dihedral labeling scheme for **oP(DA)^6**.

Conformational analysis

We have previously reported a detailed conformational analysis of the *o*-phenylenes.[28] The backbone conformation is dictated by the biaryl dihedrals (ϕ_i) shown in Fig. 1. On the NMR timescale, *o*-phenylenes longer than the pentamer undergo slow conformational exchange with respect to the internal dihedrals ϕ_2–ϕ_{n-2}.[28,29] Simple *o*-phenylenes (including the parent compounds) tend to adopt compact helical conformations with three repeat units per turn and parallel offset stacking between aromatic rings. This conformer corresponds to internal dihedrals of $\phi_i \approx -65°$ (or +65°), which we refer to as the "A" states. For example, the most stable conformer of **oP(DA)^6**, which has $\phi_2 \approx \phi_3 \approx \phi_4 \approx -65°$, is the AAA (or A_3) conformer; of course, all of the structures presented here are racemic, and there is also an enantiomeric helix with all $\phi_i \approx +65°$.

Although the dominant conformer for a simple *o*-phenylene oligomer is typically this A_{n-3} helix, minor conformers are typically observed for which the terminal rings are flipped away from the helical path. These "defects" correspond to dihedrals of

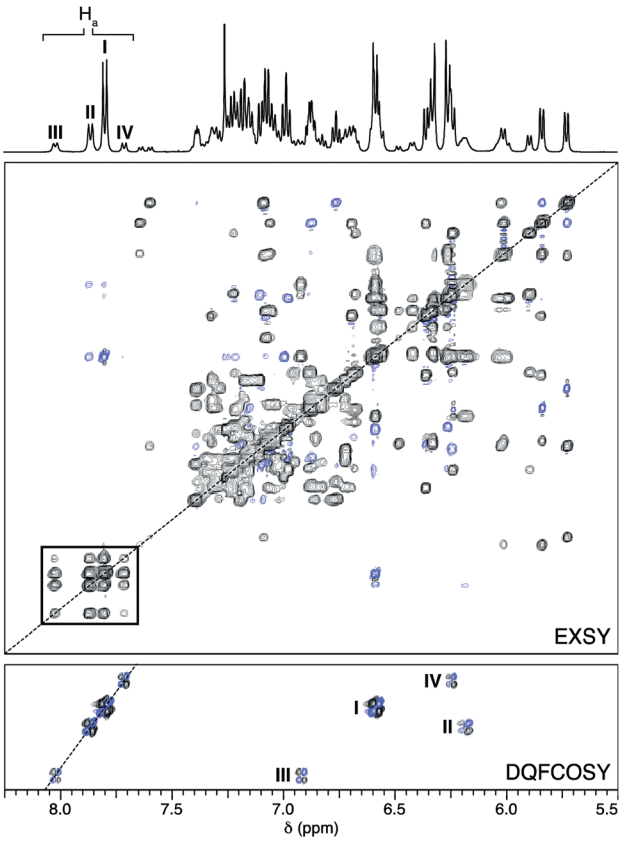

Fig. 2 Selected NMR spectra of **oP(DA)^6** (500 MHz, $CDCl_3$, 0 °C). Top: 1D ^{1}H NMR spectrum; signals corresponding to H_a in the four conformers (**I–IV**) are indicated. Middle: EXSY spectrum ($t_m \approx 0.5$ s); the box highlights the EXSY cross peaks for H_a exchanging between the four conformers. Bottom: DQFCOSY signals used to obtain chemical shifts for H_b for the four conformers.

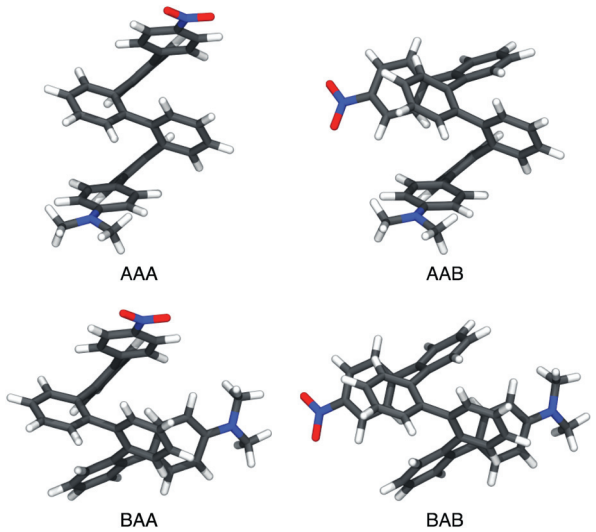

Fig. 3 Observed conformers of **oP(DA)^6**. Geometries minimized at the B3LYP/6-31+G(d,p) level.

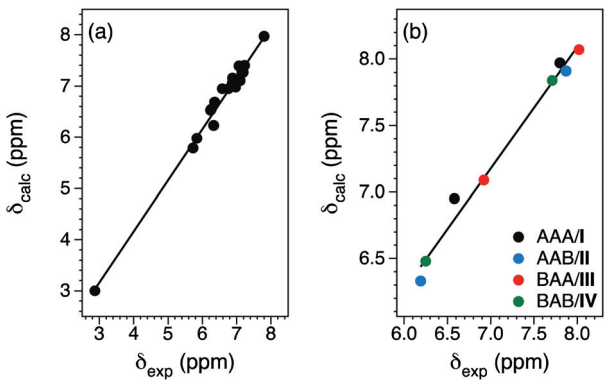

Fig. 4 Calculated (GIAO/PCM/WP04/6-31G(d)//B3LYP/6-31+G(d,p)) *vs.* experimental chemical shifts for **oP(DA)^6**. (a) Calculated for AAA geometry *vs.* **I**. (b) H_a and H_b for all four conformers.

$\phi_i \approx +130°$ (or $-130°$), which we call the "B" states. Thus, the conformational behavior at the ends of the oligomers should be particularly sensitive to substituent effects. Terminally substituted push–pull oligomers **oP(DA)^n** therefore offer an opportunity to probe whether functional groups can be used to control the conformational state of an *o*-phenylene. In particular, the hexamer **oP(DA)^6** exhibits NMR spectra that are amenable to complete assignment of the ^{1}H chemical shifts. The shorter oligomers are in fast conformational exchange on the NMR timescale. Unfortunately, the necessary two-dimensional NMR spectra for **oP(DA)^8** could not be obtained because of its poor solubility.[36]

The one-dimensional ^{1}H NMR spectrum of **oP(DA)^6** at 0 °C, shown in Fig. 2, has a set of relatively intense signals that correspond to one major species as well as a number of smaller signals. EXSY (*i.e.*, NOESY) spectroscopy demonstrates that the minor species correspond to less-populated conformational states and not impurities: cross-peaks are observed between all minor signals and corresponding signals for the major conformer. These cross-peaks are in phase with the diagonal indicating that they represent slow exchange on the NMR timescale. Four distinct conformers can be identified from the EXSY spectrum that we label **I–IV**; this is most obvious for the signals for H_a (see Fig. 1 for labeling). The relative populations of **I** : **II** : **III** : **IV** are 54 : 27 : 10 : 8 based on integration of the signals for H_a. No other conformers are observed in the spectra.

The actual geometries of these four conformers were determined using a strategy similar to our approach to the other *o*-phenylenes.[28,29] In addition to the EXSY spectra, a complete set of standard two-dimensional NMR experiments was performed, including DQFCOSY, HMQC, and HMBC (spectra given in the ESI‡). It was then possible to completely assign the chemical shifts for the major conformer **I**. By analogy with our previous work on *o*-phenylenes, we expect this conformer to correspond to the AAA geometry, shown in Fig. 3, which was optimized by DFT (B3LYP/6-31+G(d,p)). The ^{1}H chemical shifts for this geometry were then calculated using the GIAO method[37,38] and the WP04 functional[39] with the 6-31G(d) basis set, a method that has been shown to provide very accurate results with moderate computational cost.[40] As shown in Fig. 4a, a very good correlation between the calculated and experimental data is obtained. The scaled RMS error[41] of 0.12 ppm is in very good agreement with previously determined errors for the method in general[40] and *o*-phenylenes in particular: we typically take RMS errors of

less than 0.15 ppm to indicate a good match.[28,29] We therefore conclude that conformer **I** corresponds to the AAA geometry.

Unfortunately, because of the non-symmetrical substitution pattern of **oP(DA)^6**, its NMR spectra are significantly more complicated than the other *o*-phenylenes we have previously examined (which have been 2-fold symmetric).[28,29] Therefore, it was not possible to use the EXSY spectrum to directly map all of the chemical shifts for conformer **I** onto the less-populated conformers **II**, **III**, and **IV**. Fortunately, because the signals of H_a (Fig. 1) are significantly downfield from the rest of the spectrum, these protons served as a useful marker for distinguishing the different conformers. The chemical shifts of the corresponding protons H_b were then readily identified from the DQFCOSY spectrum (Fig. 2, bottom), giving two data points per conformer for use in determining their identities.

There are a total of eight possible backbone conformers for **oP(DA)^6**. However, as discussed above, our previous work on other *o*-phenylene hexamers has shown that the central bond (ϕ_3) favors the "A" state ($\phi_3 \approx 65°$), with structural variation occurring at the ends (ϕ_2 and ϕ_4). Thus, we assume here that conformers **II**, **III**, and **IV** should correspond to geometries with ϕ_3 in the A state: BAB, BAA, and AAB, shown in Fig. 3. Comparison of the calculated chemical shifts for H_a and H_b for these three geometries with the experimental data, as shown in Fig. 4b, yields the best correlation if **II** is AAB, **III** is BAA, and **IV** is BAB, with a very good overall scaled RMS error of 0.08 ppm, well below our cutoff of 0.15 ppm. We conclude therefore that our push–pull *o*-phenylenes can be broadly described by the same conformational model we have used in the past (*i.e.*, as compact helices with some conformational disorder at their ends).

Interestingly, the populations of conformers **II** (AAB) and **III** (BAA), are distinctly different (2.7 : 1). Both of these conformers consist of a single flip of one end of the oligomer out of the helical geometry; thus, the dimethylamino group more strongly favors the helical conformation. To further probe this issue, we carried out a similar conformational analysis on protonated **oP(DA)^6**, obtained by treatment with trifluoroacetic acid. NMR spectra and computational data for [**oP(DA)^6** + H^+] are given in the ESI.‡ The conformational behavior of [**oP(DA)^6** + H^+] is directly analogous to **oP(DA)^6**, except that the distribution of conformations is different: the ratio AAA : AAB : BAA : BAB is 80 : 10 : 7 : 4 (compared to 54 : 27 : 10 : 8). In other words, protonation of the dimethylamino group promotes the fully helical AAA conformer. Surprisingly, this occurs primarily by depleting the population of the AAB state: the dimethylammonium group appears to have a large effect on the conformational behavior of the opposing nitro-substituted end of the oligomer.

One of the key questions regarding the *o*-phenylenes is the origin of their preference for this particular helical structure. Standard DFT models of these compounds (B3LYP, BH&HLYP, PBE0), in our experience, have failed to predict the observed relative solution-phase conformational stabilities,[27–30] indicating that the interactions responsible for this bias are subtle. Presumably, this effect results from the well-known tendency for standard DFT functionals to poorly handle arene–arene (*e.g.*, dispersion) interactions.[42–44] Our results here demonstrate that the conformational behavior of these compounds is sensitive to substituent effects, suggesting that intramolecular forces are responsible for the folding behavior of the structures, as opposed to solvophobic[45] or excluded volume[46] effects. These substituent effects may provide an opportunity to study the specific intramolecular interactions that are significant in this class of compounds. Close inspection of the geometries in Fig. 3 suggests that the conformational distribution of these compounds may be determined by a combination of offset stacking interactions (particularly for compact helices with internal dihedrals in the A state) and edge-to-face interactions (for defects in the helix with dihedrals in the B state).[47] However, the present substituent effects are difficult to rationalize in terms of this simple model: we are not yet able to explain why protonation of the dimethylamino group affects the conformational behavior of the opposing nitro-substituted terminus. Investigation of a library of differently substituted *o*-phenylenes is currently underway in our laboratory.

UV/vis spectroscopy

To probe the interaction between the push–pull substituents through the *o*-phenylene backbone, we obtained UV/vis spectra of the **oP(DA)^n** series in a variety of solvents, shown in Fig. 5a (dichloromethane) and in the ESI (cyclohexane and methanol, Fig. S1‡). Our reference compound **oP(DA)^2** (4-dimethylamino-4′-nitrobiphenyl) exhibits a solvatochromic charge-transfer (CT) band at ~410 nm. A weak corresponding CT band (λ > 400 nm) is apparent for **oP(DA)^3**. The spectra of **oP(DA)^4**, **oP(DA)^6**, and **oP(DA)^8** have only shorter-wavelength bands that are less sensitive to solvent than the CT transitions, indicating that they correspond to excitations to non-polar locally excited states. This is further illustrated by the striking similarity between the spectra

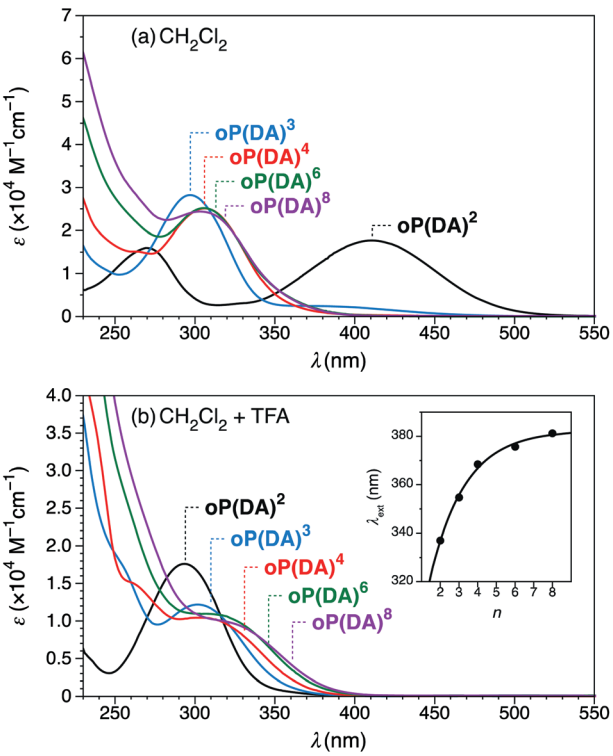

Fig. 5 (a) UV/vis spectra of **oP(DA)^n** in CH_2Cl_2. (b) UV/vis spectra in CH_2Cl_2 after addition of trifluoroacetic acid; the inset is a plot of extrapolated absorption onset against n (χ^2 = 5.56).

of **oP(DA)^4** and those of non-push–pull controls **oP(D)^4** and **oP(A)^4** (see the ESI, Fig. S2‡). Inspection of these spectra suggests that the low-energy transitions for **oP(DA)^4**, **oP(DA)^6**, and **oP(DA)^8** are localized on the nitro-functionalized end of the molecule. None of the **oP(DA)^n** series exhibits significant fluorescence, presumably due to quenching by the nitro group (**oP(A)^4** is also non-fluorescent). Compound **oP(D)^4** is highly fluorescent (in cyclohexane: λ_{max} = 407 nm, Φ_f = 0.52, see the ESI, Fig. S3‡).

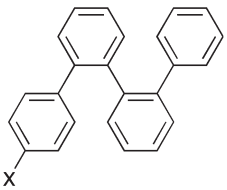

oP(D)^4: X = $N(CH_3)_2$
oP(A)^4: X = NO_2

The trends in the UV/vis spectra of the **oP(DA)^n** series are readily explained using the framework developed by Meier,[31,48–52] which considers two competing effects on λ_{max} as the length of a push–pull oligomer is increased: attenuation of the charge-transfer interaction with increasing separation (hypsochromic shifts) and extension of the conjugated backbone (bathochromic shifts). From Fig. 5a, it is clear that the charge-transfer interaction is completely absent for $n \geq 4$. The low energy transition for **oP(DA)^4** shows a slight (~10 nm) shift from the corresponding peak for **oP(DA)^3**. This presumably reflects the extension of the conjugated backbone from the trimer to the tetramer, and is in good agreement with the known effective conjugation length for unsubstituted *o*-phenylenes (n_{ecl} = 4).[29]

Consistent with the twisting of their π-systems, the charge-transfer interaction in this series of *o*-phenylenes attenuates quickly compared to similarly substituted push–pull oligomers. For example, contributions from intramolecular charge transfer for dialkylamino/nitro-substituted oligo(phenylene vinylene)s[49,51] and oligo(phenylene ethynylene)s[50] persist over 4–5 arene units. Unfortunately, examples of *p*-phenylene oligomers with similar substitution are limited, presumably because of the poor solubility of higher *p*-phenylenes.[48] However, oligomers of amino/nitro-substituted *p*-phenylenes have been reported up to *p*-quaterphenyl[53,54] and changes in λ_{max} do not reach saturation at this length, suggesting that the charge-transfer interaction through *p*-phenylenes is much stronger than in the *o*-phenylenes. Nevertheless, the observation of a charge-transfer absorption band for **oP(DA)^3** suggests moderate delocalization through the *o*-terphenyl subunits of an *o*-phenylene oligomer, and is consistent with the small but relatively long-range delocalization ($n_{ecl} \geq$ 4) of *o*-phenylenes in general.

On protonation of the dimethylamino group with trifluoroacetic acid, the charge-transfer bands for **oP(DA)^3** and **oP(DA)^4** disappear, as shown in Fig. 5b.[55] The resulting spectra show a systematic bathochromic shift with increasing *n*. Unfortunately, as with all other *o*-phenylenes we have examined, the spectra of the longer oligomers do not exhibit well-defined peaks at long wavelength; accordingly, the evolution of the spectra with *n* have been evaluated in terms of the absorption onsets λ_{ext} determined by extrapolation of the first turning points in the spectra. As expected for conjugated oligomers, the data are well fit by an empirical exponential function:[56]

$$\lambda_{ext}(n) = \lambda_\infty - \Delta\lambda e^{-b(n-1)} \quad (1)$$

where λ_∞ is the extrapolation of λ_{ext} to the polymer limit, $\Delta\lambda$ is the overall change in λ_{ext} from monomer to polymer (the effect of conjugation), and *b* quantifies the extent of conjugation (the rate at which λ_∞ is approached). The fit to eqn (1), shown in Fig. 5b (inset), gives λ_∞ = 382.4 ± 2.2 nm, $\Delta\lambda$ = 77.9 ± 5.6 nm, and *b* = 0.536 ± 0.075. The effective conjugation length (n_{ecl}) is given by:

$$n_{ecl} = \frac{\ln \Delta\lambda}{b} + 1 \quad (2)$$

From the data, the effective conjugation length for protonated **oP(DA)^n** is $n_{ecl} \approx 9$.

To better understand the electronic structures of these compounds, the frontier molecular orbitals of **oP(DA)^8** and [**oP(DA)^8** + H^+] were calculated using DFT (B3LYP/6-31+G-(d,p)) and are shown in Fig. 6. As expected, the HOMO and LUMO in **oP(DA)^8** are localized at the dimethylamino and nitro ends of **oP(DA)^8**, respectively. On protonation, the LUMO is localized on the dimethylammonium end and the HOMO is centered on the nitro end of the oligomer; consistent with the longer effective conjugation length after protonation, both frontier molecular orbitals are delocalized further into the chain.

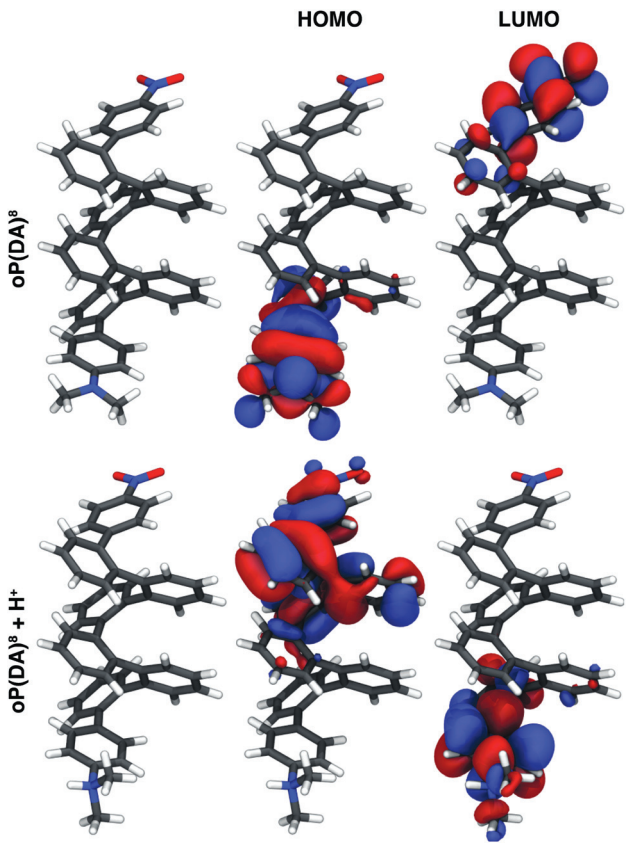

Fig. 6 Frontier molecular orbitals for **oP(DA)^8** (top) and protonated **oP(DA)^8** (bottom) calculated at the B3LYP/6-31+G(d,p) level. Orbitals are plotted with isosurface values of 0.02.

Interestingly, the effective conjugation length for the protonated **oP(DA)″** series is more than twice that of the parent *o*-phenylenes ($n_{ecl} \approx 4$), and similar to our previously reported methoxy-substituted series ($n_{ecl} \approx 8$). Clearly, a series of "pull–pull" oligomers (*i.e.*, without a direct structural analogy to a simple polymer) cannot be directly compared to a uniformly functionalized series. However, this result does underscore the sensitivity of the conjugation length to substituent effects. While we were unable to locate many direct analogies to these compounds, it is interesting to note that in Meier's amino/nitro-functionalized oligo(phenylene vinylene)s, the conjugation length on protonation is not any longer than the analogous (unfunctionalized) PPV oligomers. This sensitivity of the π-system to substituent effects suggests that the *o*-phenylenes, and perhaps other weakly conjugated systems, may have use in certain applications for conjugated oligomers where a direct increase in absorption (or emission) wavelength is not needed, such as molecular wires.

Conclusions

In summary, we have prepared a series of push–pull-substituted *o*-phenylene oligomers **oP(DA)″**. These compounds have allowed us to show that the conformational states of *o*-phenylene oligomers are sensitive to substituent effects, suggesting that subtle intramolecular forces must be responsible for their folding behavior. UV/vis spectra demonstrate that intramolecular charge-transfer interactions are observable through *o*-terphenyl linkages, but not beyond. On protonation, however, a significant extension of the effective conjugation length compared to parent *o*-phenylene is observed.

Experimental

General

Unless otherwise noted, all starting materials, reagents, and solvents were purchased from commercial sources and used without further purification. Anhydrous THF was obtained by distillation from sodium–benzophenone. Anhydrous CH_2Cl_2 was obtained by distillation from CaH_2. Melting points were determined using a Thermal Analysis Q20 differential scanning calorimeter at a heating rate of 10 °C min^{-1}. NMR spectra were measured for $CDCl_3$ solutions using Bruker Avance 300 MHz or 500 MHz NMR spectrometers. Chemical shifts are reported in δ (ppm) relative to TMS, with the residual solvent protons used as internal standards. Measured temperatures for variable temperature NMR experiments are uncorrected. Low resolution ESI mass spectra were recorded on Bruker Esquire ESI mass spectrometer. High resolution ESI mass spectra were obtained at the Ohio State Mass Spectrometry and Proteomics Facility. MALDI spectra were acquired on a Bruker Ultraflex MALDI spectrometer using dithranol as the matrix. UV/vis spectra were recorded using a Perkin Elmer Lambda 35 spectrophotometer. Fluorescence emission/excitation spectra were recorded using a Perkin Elmer LS 55 fluorescence spectrophotometer, and are corrected for emission.[57] The quantum yield of **oP(D)^4** was determined in nitrogen-sparged cyclohexane according to the standard procedure: five solutions of varying concentrations were used and a good linear fit ($R^2 \geq 0.99$) was observed when integrated fluorescence intensity was plotted against absorbance. 9,10-diphenylanthracene in cyclohexane ($\Phi_f = 0.91$) was used as the standard, which was cross-checked against quinine bisulfate ($\Phi_f = 0.54$). Absorbances of the sample solutions were kept below 0.10 (10 mm cuvettes) to avoid the inner filter effect. Measurements were performed at room temperature, with both sample and reference solutions excited at the same wavelength (275 nm). DFT calculations were carried out using Gaussian 09 (Rev. B.01)[58] on Miami University's Redhawk computer cluster. Calculated geometries and orbitals were visualized using VMD.[59]

Synthesis of oP(A)″-OH and oP(A)″-OTf

oP(A)^3-OH and **oP(A)^3-OTf**: A Schlenk vacuum tube was charged with 1-bromo-4-nitrobenzene (3.10 g, 15.3 mmol), **1** (2.00 g, 10.2 mmol), $Pd(OAc)_2$ (229 mg, 1.02 mmol), SPhos (502 mg, 1.22 mmol), and K_3PO_4 (5.41 g, 25.5 mmol), then evacuated and backfilled with argon (3×). Anhydrous THF (28 mL) was added followed by deionized water (7 mL). The reaction mixture was degassed by three freeze-pump-thaw cycles, then sealed and heated at 85–90 °C for 24 h. The mixture was then cooled, acidified with HCl, diluted with EtOAc, and washed with water and brine. The organic layer was dried over Na_2SO_4, filtered, and concentrated. The crude **oP(A)^3-OH** was then passed through a plug of silica gel (4 : 1 hexanes–EtOAc) and used without further purification. A stirred solution of the **oP(A)^3-OH** (2.15 g, 7.38 mmol) in anhydrous CH_2Cl_2 (25 mL) was treated with pyridine (1.2 mL, 14.76 mmol), and the reaction mixture cooled to 0 °C. Trifluoromethanesulfonic anhydride (1.86 ml, 11.07 mmol) was added dropwise. The reaction was allowed to warm slowly to room temperature overnight. The reaction mixture was diluted with EtOAc and washed with 1 M HCl, water, and brine, then dried over Na_2SO_4, filtered, and concentrated. Purification by flash chromatography (9 : 1 hexanes–EtOAc) followed by recrystallization from abs. ethanol gave 2.78 g (6.57 mmol, 64%) of **oP(A)^3-OTf** as off-white crystals: m.p. 136.1 °C; ^{1}H NMR ($CDCl_3$, 500 MHz) δ 7.13 (d, 1H, J = 2.3 Hz), 7.28 (m, 2H), 7.38 (m, 3H), 7.46 (m, 2H), 7.54 (m, 2H), 8.06 (m, 2H); ^{13}C NMR ($CDCl_3$, 125 MHz) δ 118.2 (q, J = 320.9 Hz), 121.8, 123.2, 128.5, 128.7, 129.2, 129.7, 130.0, 130.2, 131.7, 132.7, 133.9, 134.5, 139.4, 146.5, 146.8, 147.7; MS (ESI) calcd for $C_{19}H_{12}F_3NNaO_5S$ ($M + Na^+$) 446.0, found 446.1.

oP(A)^5-OH and **oP(A)^5-OTf**: The procedure for **oP(A)^3-OTf** was followed using **oP(A)^3-OTf** (2.50 g, 5.90 mmol) as the starting material. **oP(A)^5-OH** was eluted through a plug of silica gel (4 : 1 hexanes–EtOAc). Purification by flash chromatography (7 : 3 hexanes–CH_2Cl_2) gave 2.98 g (5.17 mmol, 88%) of **oP(A)^5-OTf** as a pale yellow foam: m.p. 163.0 °C; ^{1}H NMR complex due to slow conformational exchange, see the ESI;‡ MS (ESI) calcd for $C_{31}H_{20}F_3NNaO_5S$ ($M + Na^+$) 598.1, found 598.1.

oP(A)^7-OH and **oP(A)^7-OTf**: The procedure for **oP(A)^3-OTf** was followed using **oP(A)^5-OTf** (2.00 g, 3.47 mmol) as the starting material. **oP(A)^7-OH** was eluted through a plug of silica gel (4 : 1 hexanes–EtOAc). Purification by flash chromatography (7 : 3 hexanes–CH_2Cl_2) gave 2.17 g (2.98 mmol, 86%) of

oP(A)^7-OTf as an off-white foam: m.p. 205.2 °C; ^{1}H NMR complex due to slow conformational exchange, see the ESI;‡ MS (ESI) calcd for $C_{43}H_{28}F_3NNaO_5S$ (M + Na^+) 750.2, found 750.2.

Synthesis of oP(DA)^n

General procedure: A Schlenk vacuum tube was charged with **oP(A)$^{n-1}$-OTf** (1.00 mmol), 4-(dimethylamino)phenylboronic acid (198 mg, 1.20 mmol), $Pd(OAc)_2$ (44.9 mg, 0.20 mol), SPhos (98.5 mg, 0.24 mmol), and K_3PO_4 (849 mg, 4.00 mmol), then evacuated and backfilled with argon (3×). Anhydrous THF (2.0 mL) was added followed by deionized water (0.5 mL). The reaction mixture was degassed by three freeze–pump–thaw cycles, then sealed and heated at 80–85 °C overnight. The reaction mixture was then cooled, diluted with EtOAc (20 mL), and washed with water, acidifying the aqueous layer with 1 M HCl (15 mL). The aqueous layer was extracted with EtOAc and the combined organic layers washed with water and brine, dried over $MgSO_4$, filtered, and concentrated.

oP(DA)^4: Purification by flash chromatography (CH_2Cl_2) gave 210 mg (0.53 mmol, 53%) of **oP(DA)^4** as a red solid, which was recrystallized from abs. ethanol prior to further analysis: m.p. 229.0 °C; ^{1}H NMR ($CDCl_3$, 500 MHz) δ 2.90 (s, 6H), 6.39 (m, 4H), 6.71 (m, 2H), 7.14 (m, 2H), 7.34 (m, 2H), 7.39 (td, 1H, J = 7.6, 1.3 Hz), 7.43 (m, 1H), 7.49 (td, 1H, J = 7.3, 1.3 Hz,), 7.53 (dd, 1H, J = 7.5, 1.3 Hz,), 7.84 (m, 2H); ^{13}C NMR ($CDCl_3$, 125 MHz) δ 40.8, 112.1, 122.6, 126.7, 127.7, 128.2, 128.8, 129.7, 129.8, 129.96, 130.03, 131.6, 132.0, 138.7, 138.9, 141.0, 146.1, 148.2, 149.3; MS (MALDI) calcd for $C_{26}H_{21}N_2O_2$ (M − H) 393.16, found 392.88; HRMS (ESI) calcd for $C_{26}H_{23}N_2O_2$ (M + H^+) 395.1681, found 395.1691.

oP(DA)^6: Purification by flash chromatography (toluene) gave 284 mg (0.52 mmol, 52%) of **oP(DA)^6** as a deep yellow solid, which was recrystallized from abs. ethanol prior to further analysis: m.p. 224.7 °C; ^{1}H NMR complex due to slow conformational exchange, see the Results and discussion section and the ESI;‡ MS (MALDI) calcd for $C_{38}H_{29}N_2O_2$ (M − H) 545.22, found 545.14; HRMS (ESI) calcd for $C_{38}H_{31}N_2O_2$ (M+H^+) 547.2386, found 547.2393.

oP(DA)^8: Purification by flash chromatography ($CHCl_3$) gave 211 mg (0.54 mmol, 54%) of **oP(DA)^8** as a light yellow solid: m.p. 303.8 °C; ^{1}H NMR complex due to slow conformational exchange, see the ESI;‡ MS (MALDI) calcd for $C_{50}H_{37}N_2O_2$ (M − H) 697.29, found 697.28; HRMS (ESI) calcd for $C_{50}H_{38}N_2NaO_2$ (M + Na^+) 721.2831, found 721.2854.

Acknowledgements

Primary support from the National Science Foundation (CHE-0910477) is gratefully acknowledged. Gaussian 09 was purchased with the assistance of the Air Force Office of Scientific Research (FA9550-10-1-0377), and the MALDI mass spectrometer was purchased with the assistance of the NSF (CHE-0839233).

Notes and references

1 S. H. Gellman, *Acc. Chem. Res.*, 1998, **31**, 173–180.
2 D. J. Hill, M. J. Mio, R. B. Prince, T. S. Hughes and J. S. Moore, *Chem. Rev.*, 2001, **101**, 3893–4011.
3 J. J. L. M. Cornelissen, A. E. Rowan, R. J. M. Nolte and N. A. J. M. Sommerdijk, *Chem. Rev.*, 2001, **101**, 4039–4070.
4 *Foldamers: Structure, Properties, and Applications*, ed. S. Hecht and I. Huc, Wiley-VCH, Weinheim, 2007.
5 E. Yashima, K. Maeda, H. Iida, Y. Furusho and K. Nagai, *Chem. Rev.*, 2009, **109**, 6102–6211.
6 G. Guichard and I. Huc, *Chem. Commun.*, 2011, **47**, 5933–5941.
7 J.-m. Suk and K.-S. Jeong, *J. Am. Chem. Soc.*, 2008, **130**, 11868–11869.
8 K. Yamato, L. Yuan, W. Feng, A. J. Helsel, A. R. Sanford, J. Zhu, J. G. Deng, X. C. Zeng and B. Gong, *Org. Biomol. Chem.*, 2009, **7**, 3643–3647.
9 M. Waki, H. Abe and M. Inouye, *Angew. Chem., Int. Ed.*, 2007, **46**, 3059–3061.
10 H. Juwarker, J.-m. Suk and K.-S. Jeong, *Chem. Soc. Rev.*, 2009, **38**, 3316–3325.
11 Q. Gan, Y. Ferrand, C. Bao, B. Kauffmann, A. Grélard, H. Jiang and I. Huc, *Science*, 2011, **331**, 1172–1175.
12 R. B. Prince, S. A. Barnes and J. S. Moore, *J. Am. Chem. Soc.*, 2000, **122**, 2758–2762.
13 V. Percec, J. G. Rudick, M. Peterca and P. A. Heiney, *J. Am. Chem. Soc.*, 2008, **130**, 7503–7508.
14 H.-J. Kim, E. Lee, H.-S. Park and M. Lee, *J. Am. Chem. Soc.*, 2007, **129**, 10994–10995.
15 K. Miwa, Y. Furusho and E. Yashima, *Nat. Chem.*, 2010, **2**, 444–449.
16 K. Maeda and E. Yashima, *Top. Curr. Chem.*, 2006, **265**, 47–88.
17 R. Liu, M. Shiotsuki, T. Masuda and F. Sanda, *Macromolecules*, 2009, **42**, 6115–6122.
18 P. Rivera-Fuentes, J. L. Alonso-Gómez, A. G. Petrovic, F. Santoro, N. Harada, N. Berova and F. Diederich, *Angew. Chem., Int. Ed.*, 2010, **49**, 2247–2250.
19 R. W. Sinkeldam, F. J. M. Hoeben, M. J. Pouderoijen, I. De Cat, J. Zhang, S. Furukawa, S. De Feyter, J. A. J. M. Vekemans and E. W. Meijer, *J. Am. Chem. Soc.*, 2006, **128**, 16113–16121.
20 M. Wolffs, N. Delsuc, D. Veldman, N. Vân Anh, R. M. Williams, S. C. J. Meskers, R. A. J. Janssen, I. Huc and A. P. H. J. Schenning, *J. Am. Chem. Soc.*, 2009, **131**, 4819–4829.
21 G. Wittig and G. Lehmann, *Chem. Ber.*, 1957, **90**, 875–892.
22 P. Kovacic and J. S. Ramsey, *J. Polym. Sci., Part A-1*, 1969, **7**, 111–125.
23 P. Kovacic, J. T. Uchic and L.-C. Hsu, *J. Polym. Sci., Part A-1*, 1967, **5**, 945–964.
24 S. Ozasa, Y. Fujioka, M. Fujiwara and E. Ibuki, *Chem. Pharm. Bull.*, 1980, **28**, 3210–3222.
25 A. J. Blake, P. A. Cooke, K. J. Doyle, S. Gair and N. S. Simpkins, *Tetrahedron Lett.*, 1998, **39**, 9093–9096.
26 E. Ohta, H. Sato, S. Ando, A. Kosaka, T. Fukushima, D. Hashizume, M. Yamasaki, K. Hasegawa, A. Muraoka, H. Ushiyama, K. Yamashita and T. Aida, *Nat. Chem.*, 2011, **3**, 68–73.
27 J. He, J. L. Crase, S. H. Wadumethrige, K. Thakur, L. Dai, S. Zou, R. Rathore and C. S. Hartley, *J. Am. Chem. Soc.*, 2010, **132**, 13848–13857.
28 C. S. Hartley and J. He, *J. Org. Chem.*, 2010, **75**, 8627–8636.
29 S. M. Mathew and C. S. Hartley, *Macromolecules*, 2011, **44**, 8425–8432.
30 C. S. Hartley, *J. Org. Chem.*, 2011, **76**, 9188–9191.
31 H. Meier, *Angew. Chem., Int. Ed.*, 2005, **44**, 2482–2506.
32 S. Ishikawa and K. Manabe, *Chem. Commun.*, 2006, 2589–2591.
33 S. Ishikawa and K. Manabe, *Chem. Lett.*, 2006, **35**, 164–165.
34 Q. J. Zhou, K. Worm and R. E. Dolle, *J. Org. Chem.*, 2004, **69**, 5147–5149.
35 S. D. Walker, T. E. Barder, J. R. Martinelli and S. L. Buchwald, *Angew. Chem., Int. Ed.*, 2004, **43**, 1871–1876.
36 **oP(DA)^8** exhibits insufficient solubility for 2D NMR experiments in deuterated chloroform, benzene, acetone, DMSO, and trifluoroethanol.
37 R. Ditchfield, *Mol. Phys.*, 1974, **27**, 789–807.
38 K. Wolinski, J. F. Hinton and P. Pulay, *J. Am. Chem. Soc.*, 1990, **112**, 8251–8260.
39 K. W. Wiitala, T. R. Hoye and C. J. Cramer, *J. Chem. Theory Comput.*, 2006, **2**, 1085–1092.
40 R. Jain, T. Bally and P. R. Rablen, *J. Org. Chem.*, 2009, **74**, 4017–4023.
41 As in ref. 40, the δ_{calc} values are scaled by $\delta'_{calc} = (\delta_{calc} - b)/m$, where m is the slope and b is the intercept from the plot of δ_{calc} *vs.* δ_{exp}.
42 S. Kristyán and P. Pulay, *Chem. Phys. Lett.*, 1994, **229**, 175–180.
43 A. Godfrey-Kittle and M. Cafiero, *Int. J. Quantum Chem.*, 2006, **106**, 2035–2043.

44 S. Tsuzuki and H. P. Lüthi, *J. Chem. Phys.*, 2001, **114**, 3949–3957.
45 J. C. Nelson, J. G. Saven, J. S. Moore and P. G. Wolynes, *Science*, 1997, **277**, 1793–1796.
46 Y. Snir and R. D. Kamien, *Science*, 2005, **307**, 1067–1067.
47 C. A. Hunter and J. K. M. Sanders, *J. Am. Chem. Soc.*, 1990, **112**, 5525–5534.
48 S. Kim, A. Oehlhof, B. Beile and H. Meier, *Helv. Chim. Acta*, 2009, **92**, 1023–1033.
49 H. Meier, J. Gerold, H. Kolshorn and B. Mühling, *Chem.–Eur. J.*, 2004, **10**, 360–370.
50 H. Meier, B. Mühling and H. Kolshorn, *Eur. J. Org. Chem.*, 2004, 1033–1042.
51 H. Meier, J. Gerold, H. Kolshorn, W. Baumann and M. Bletz, *Angew. Chem., Int. Ed.*, 2002, **41**, 292–295.
52 H. Meier, R. Petermann and J. Gerold, *Chem. Commun.*, 1999, 977–978.
53 L. T. Cheng, W. Tam, S. R. Marder, A. E. Stiegman, G. Rikken and C. W. Spangler, *J. Phys. Chem.*, 1991, **95**, 10643–10652.
54 R. W. H. Berry, P. Brocklehurst and A. Burawoy, *Tetrahedron*, 1960, **10**, 109–117.
55 Identical results were obtained using a drop of conc. HCl.
56 H. Meier, U. Stalmach and H. Kolshorn, *Acta Polym.*, 1997, **48**, 379–384.
57 D. Pfeifer, K. Hoffmann, A. Hoffmann, C. Monte and U. Resch-Genger, *J. Fluoresc.*, 2006, **16**, 581–587.
58 M. J. Frisch, *et al.*, *GAUSSIAN 09 (Revision B.01)*, Gaussian, Inc., Wallingford, CT.
59 W. Humphrey, A. Dalke and K. Schulten, *J. Mol. Graphics*, 1996, **14**, 33–38.